SERI/TR-9-8074-1
UC CATEGORY: 60

FOURTH ANNUAL PROGRESS REPORT ON THE ELECTROFLUID DYNAMIC WIND GENERATOR

FINAL REPORT FOR THE PERIOD
1 APRIL 1979-31 AUGUST 1980

AUGUST 1981

JOHN E. MINARDI
MAURICE O. LAWSON
FRANK L. WATTENDORF

UNIVERSITY OF DAYTON
DAYTON, OHIO

PREPARED UNDER SUBCONTRACT
NO. XH-9-8074-1
FOR THE
Solar Energy Research Institute
A Division of Midwest Research Institute

1617 Cole Boulevard
Golden, Colorado 80401

Prepared for the
U.S. Department of Energy
Contract No. EG-77-C-01-4042

SERI TECHNICAL MONITOR:

RICHARD MITCHELL

FOREWORD

The research described in this report was performed under DOE Contract No. EY-76-S-02-4130, for the Wind Systems Branch, U.S. Department of Energy (DOE), and for the Solar Energy Research Institute (SERI), subcontract number XH-9-8074-1. The work was accomplished between 1 April 1979 and 31 August 1980. Mr. Lou Divone was Program Manager for the Wind Systems Branch and Mr. Richard Mitchell was Project Manager for SERI.

The authors wish to acknowledge the many personnel at the University of Dayton Research Institute who assisted in this program: Mr. D. H. Whitford, Dr. R. P. Braden, Mr. F. J. Pestian, and Mr. R. Ely. A special note of appreciation is due Miss Norma Harting for typing and for providing general assistance in preparation of this report.

EXECUTIVE SUMMARY

INTRODUCTION

Conventional wind energy systems are limited in wind turbine diameter by allowable rotor stresses at power levels of several megawatts. In contrast, the Electrofluid Dynamic (EFD) wind driven generator has no fundamental limits on cross-sectional area. It is a direct energy conversion device which employs unipolar charged particles transported by the wind against a retarding voltage gradient to a high potential. As no moving parts are exposed to the wind, extremely large power units may be feasible.

In an EFD generator, charge particles of one polarity are seeded into a flowing neutral gas. Viscous interactions with neutral molecules drive the charged particles against an electrical potential and produce dc power of low current density and very high voltage. In the first year's research a substantial theory of the operation of EFD wind driven generators was established as well as the identification of three major milestones:

1. Development of a laboratory method for the production of low mobility charged droplets in adequate numbers that are suitable for the testing of generator designs.
2. Verification of generator performance theory.
3. Demonstration of an energy economic method of producing and distributing low mobility charged droplets.

Milestones (1) and (2) above were accomplished during the 1977-78 calendar years so that the primary emphasis of the past year's research effort has been directed at the attainment of the last milestone (3 above).

THEORETICAL STUDIES

Studies were conducted with regard to the problem of the distribution of small amounts of water required as charge carriers, over a large frontal area. For example, in low wind velocity regions it was found that approximately four (4) grams of water per second per square meter of generator frontal area would be required. Calculations show that for a continuous-slot emitter of water, the height of the slot required is only 0.6 microns. This is an impractically small size. Replacing the slot with distributed circular holes also resulted in impractically small diameters. Thus some other approach was needed.

In addition, earlier work had shown that the application of electrohydrodynamic spraying was incompatible with the small charge-to-mass-ratio droplets necessary for practical implementation of the EFD wind generator principle. Another well known charging process is induction. However, in applying the induction process the required breakup of the water into micron or submicron droplets would require another process to supply the high surface tension energies of very small droplets.

A process that can greatly augment the small volume flow of water needed for the formation of droplets and also can provide the high surface tension energies of submicron size droplets is the production of thin wall bubbles. In the body of the report we present considerations for the beneficial effect of using bubbles on the emitter slot widths. Analyses are also presented for applying induction charging to bubbles and we determine limiting bubble diameters for electrical stability of bubbles with desirable ratios of charge to water mass. Studies are also made as to the applicability of bubbles to serve as charge carriers, and to participate in the energy conversion process. These studies indicate that a method for breaking up the charged bubbles shortly after or during their formation is required.

EXPERIMENTAL INVESTIGATIONS

The experimental program consisted of tests of a large electrode geometry and the investigation of bubble generator concepts. Both of these aspects are discussed below.

DESIGN AND TESTING OF LARGE ELECTRODE GEOMETRY

The experimental investigations of the use of bubbles for the proper distribution and charging of water to provide energy-economic, low-mobility, charged droplets has required the design and fabrication of a new large electrode generator test apparatus. It was desired to reduce the number of flow channels from eleven to three, where, for the energy economic charging experiments, only the center channel would be seeded with charged bubbles. This would reduce the complexity of the test setup, yet provide representative flow conditions. The entrance electrode diameters were scaled to larger diameters by the factor 3.2 and the generator frontal area was held constant.

The research plan included the testing of the large electrode design with the previously developed droplet forming and charging system to provide base levels of maximum current. This method, although not energy economic, had provided design levels of current of the required low mobility and had allowed the successful verification of EFD wind generator theory. Maximum current experiments employing the large electrode geometry yielded values of about 60 percent of those of the small-diameter array tested earlier. It is not known at this time whether this lower level of current corresponds to a theoretical limit but the possibility of this being the case should be examined using the field-solution computer program. However, even with the lower current levels the rig was suitable for use in testing of the bubble concept.

DESIGN AND TESTING OF BUBBLE GENERATOR AND EMITTER ELECTRODE

A review of commercial-foam generators for fire fighting applications showed that the smallest size commercial unit is far

too large for the present application. This circumstance led to the design of a bubble generator having a great amount of flexibility with regard to volume flow and bubble characteristics. Two different geometry emitter electrodes having airfoil shapes were designed. One has a single bubble emitting slot in the trailing edge and the second has two slots, one on either surface of the emitter near the trailing edge. In their operation, an electric field charges the bubbles by inducing charge on the surface of the bubbles as they leave the metal surface.

Initial tests of the two slot emitter electrode produced satisfactory level of emitter currents. The theoretical investigation earlier discussed showed that the charged bubbles would be required to burst into small size droplets in order to provide satisfactory low mobility charged droplets. This will require additional experiments and perhaps simpler, more basic test geometries.

FUTURE PROGRAM PLANS

Theoretical and experimental findings support the applicability of forming charged, thin-walled bubbles as a method of overcoming the two major problems of distributing extremely small amounts of water and of providing the high ratio of surface tension energy to water mass that the production of micron and submicron droplets requires. Moreover, the energy economic studies conducted showed conclusively that the bubbles must be caused to burst into micron size droplets upstream of the energy conversion section of the generator. In view of the above, research is needed in the production, charging, and disintegration of thin wall bubbles as a source of suitably charged micron and submicron sized droplets.

TABLE OF CONTENTS

SECTION 1
INTRODUCTION

A major performance need presently exists in the large power wind systems being developed. This is the capability of an individual unit to generate power corresponding to a sizable fraction of that of a steam plant generator system. Conventional wind energy systems are limited in wind turbine diameter by allowable rotor stresses at power levels of several megawatts. In contrast, the Electrofluid Dynamic (EFD) wind driven generator has no fundamental limits on size. It is a direct energy conversion device which employs unipolar charged particles transported by the wind against a retarding voltage gradient to a high potential. Hence, since few limitations on area exist, one may be able to build extremely large power units.

Previous reports published in this research effort present a substantial theory for the performance of EFD wind driven generators as well as the experimental verification of that theory.

In an EFD generator, charged particles of one polarity are seeded into a flowing neutral gas. Viscous interactions drive the charged particles against an electrical potential and produce dc power. Typically, the EFD generator develops high voltages and low current densities. As shown on Figure 1, the generator consists of the following parts:

1. A mechanism for producing charged colloidal-sized particles.

2. An inlet electrode which also serves as an attractor electrode.

3. A collector electrode.

4. A high voltage power supply.

5. A control system.

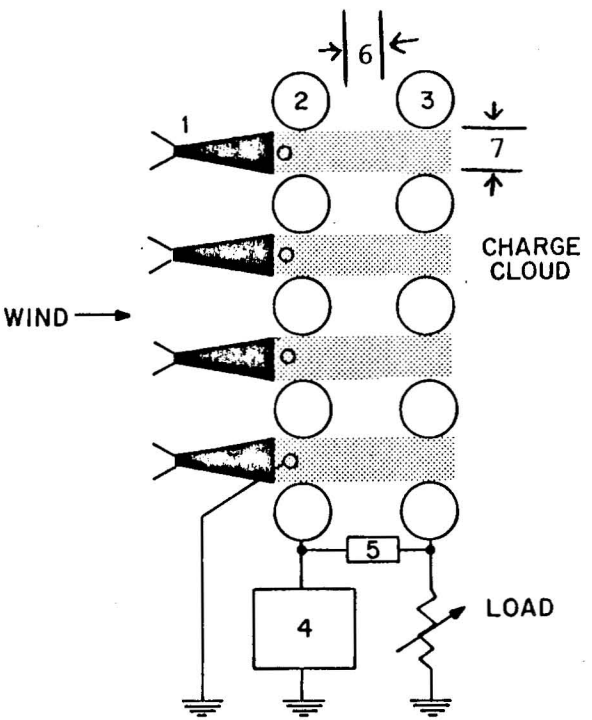

1 COLLOID CHARGING SYSTEM
2 INLET/ATTRACTOR ELECTRODE
3 COLLECTOR ELECTRODE
4 HIGH VOLTAGE POWER SUPPLY
5 FEEDBACK CONTROL SYSTEM
6 CONVERSION SECTION
7 FLOW CHANNEL

Figure 1. Schematic of an EFD Wind Driven Generator.

6. A conversion section.

7. A flow channel.

The high voltage power supply places the attractor electrode at a high dc voltage relative to the particle producing electrode. Charged particles of one sign produced by the charging system are swept past the attractor electrode into the conversion section by the moving air toward the collector electrode. The collector voltage depends on the load and current, but the charged particles must be driven up a potential hill in the conversion section by the neutral particles of the moving air. Thus, electrical power is generated directly by the moving air with no moving parts required. The feedback control system senses the voltage on the collector and adjusts the attractor voltage, thereby controlling the output current in order to match electrical output to wind power, while providing constant output voltage.

This report presents additional theoretical studies and results of experiments which focus on the single remaining research problem area: the energy economic production of low mobility charged droplets.

Section 3 presents a summary of progress in previous years. Section 4 presents current progress made in the theoretical studies, and Section 5 discusses the experimental program and presents the experimental results. Finally, Section 6 discusses future program plans.

SECTION 2
SUMMARY OF PREVIOUS YEARS PROGRESS

Significant progress was reported in the first three years of the research program toward the objective of attaining practical EFD wind driven generators. Some of the major accomplishments were:

1. Development of a substantial theory which has broadened the classical one-dimensional anlaysis and extended its application to the performance of wind driven generators.[1,2]

2. Computer mapping of the electrical field for various generator geometries.[3]

3. Construction of a small wind tunnel with a test section of nearly one meter by one meter for testing EFD wind driven generator configurations.[4]

4. Fabrication of a variable geometry test generator.[5]

5. Prediction of optimum generator performance for test electrode arrays over a range of geometries.[6]

6. Identification of energy requirements in the production of charged droplets.[7]

7. Identification of superior generator performance regimes by mapping in the charged droplet mobility-radius plane.[8]

8. Identification of experimental problem areas.[9]

9. Demonstration of progressive geometric increase in generator power by the elimination of experimental problem areas.[10]

10. Identification of problem areas that need solution for the practical application of EFD wind driven generators.[11]

11. Development of the Faraday Cage Collector whose performance is sensitive only to Poisson fields[12] (fields resulting from space charges inside the collector).

12. Fabrication of a test facility for charged droplet production.[13]

13. Development of a laboratory method for the production of low mobility charged droplets in adequate numbers that are suitable for the testing of generator designs.[14]

14. Experimental verification of generator performance theory.[15]

The last two accomplishments listed above represent the attainment of milestones which were established in the original long-range program plan. The effort during this past year has been directed toward the attainment of the third and only remaining milestone: demonstrating an energy economic method of producing and distributing low mobility charged droplets.

In the following sections of this report, the accomplishments of the past year's effort toward the attainment of the final milestone will be discussed.

SECTION 3
THEORETICAL STUDIES

3.1 INTRODUCTION

The theoretical efforts conducted during the last year have focused on the two major problem areas in the production of energy economic charged droplets. The first is the distribution of an extremely low flow rate of water per unit frontal area of the EFD wind generator; and the second is the achievement of a satisfactorily low charge to mass ratio of the charged droplets. With regard to the latter, it was shown in the previous effort that the electrohydrodynamic (EHD) spraying process produces charged droplets which have a far too high charge to mass ratio. The EHD spraying process has been shown to correspond to Vonnegut and Neubauer's droplet energy minimization analysis[16]. One major result of this analysis is that the ratio of capacitive energy to surface tension energy is equal to 1/2 for all radius droplets. However, the surface tension energy required for small drops is very high. Therefore, the capacitive energy in EHD spraying processes is also high since it is 1/2 of the surface tension energy. This amount of energy yields very high charge to mass ratios and, consequently, high mobility in the droplet size of interest for EFD wind generators, i.e., equal to or smaller than one micron radius[1].

Induction charging of jets or sheets of water would appear to be an ideal method to produce energy economic charged droplets since the charging rate is proportional to the local field strength where the water exits. However, the problem mentioned earlier, that of the distribution of a low mass flow rate of water per unit frontal area, must be solved first.

3.2 THE CHARGED DROPLET WATER DISTRIBUTION PROBLEM

Since the water distribution problem will be most severe for a low wind velocity operating condition, we will consider

that case as an example. An EFD generator designed to operate in a five meter per second wind may produce about 35 watts of power per square meter frontal area (see Figure 2 taken from Reference (1)). Such a generator will probably be designed to produce power at, or above 300,000 volts, and the charge to water mass ratio may be 0.03 C/kg or even somewhat higher.[17] Based on these values, the water mass flow rate (per unit of frontal area) which corresponds to a volume flow rate of 4 cc/s.

$$\dot{m}_w = \frac{35 \text{ watts/m}^2}{.03 \frac{c}{kg_{(w)}} \times 3 \times 10^5 v}$$

$$= .0039 \frac{kg}{s \times m^2}$$

In Figure 2 the entrance electrodes diameter was selected as 12 inches or 0.305 m. Let us assume that the curve parameter value of "a" is equal to 2.34, (the lateral spacing divided by electrode diameter).

For this value of "a" the electrode spacing, S, is:

$$S = D \times a = .3048 \times 2.34 = .713 \text{ m}$$

Thus, one square meter of frontal area can be achieved in a length of 1.4 m (i.e., L = 1/S so that A = L S = 1 M^2).

If we assume one water emitter per channel, the water flow of 4 cc/s should be distributed uniformly over the length of 1.4 meters for each square meter of generator array. If we assumed a continuous slit opening and a water flow velocity equal to the wind velocity (5 meters per second), then the slot height, Δh, is

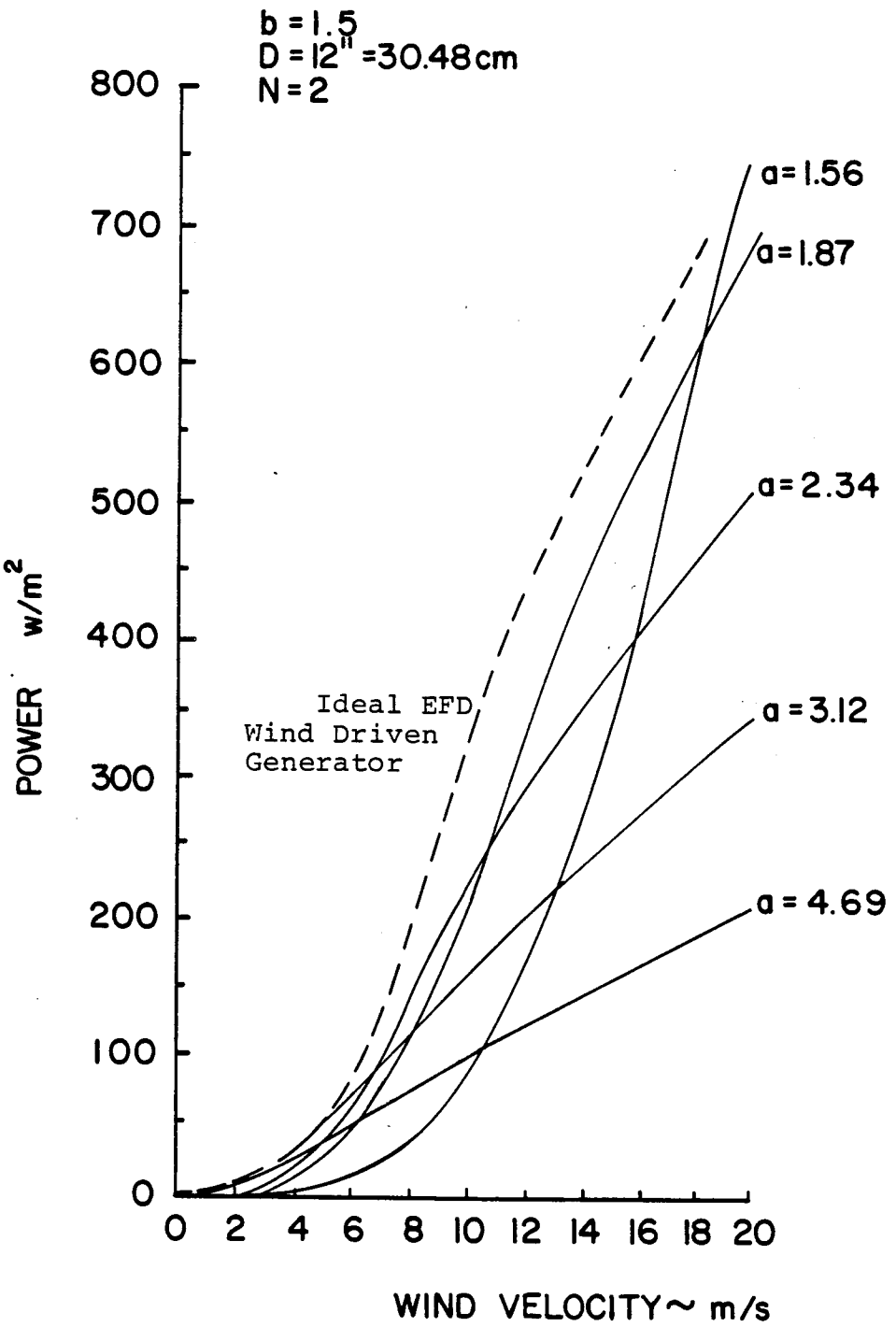

Figure 2. Theoretical Power Output of a Full Size EFD Wind Driven Generator for Various Electrode Spacings.

$$\Delta h = \frac{4 \times 10^{-6} \frac{m^3}{s}}{5 \frac{m}{s} \times 1.4 \text{ m}} \simeq 6 \times 10^{-7} \text{ m}$$

This is an impractically small size for a water emitter opening.

For the case of applying distributed circular holes in lieu of a slit opening for the water emitter electrode, their maximum diameter will be limited by effects of the nonuniformity of the Poisson field, and by the magnitude of the charge to mass ratio, A cylinder of charge moving with the local air velocity will be limited in diameter to about 1.8×10^{-6} meters for the case that the local Poisson radial field is taken as 1.5×10^{6} V/m, corresponsing to one half the breakdown strength of air. Due to the conductivity of the water, and possible narrowing down of the jet, the largest size diameter hole could be possibly somewhat larger than 1.8×10^{-6} m, but even a hole larger by the factor of 10 or so would be impractical for the present application. Thus, some other approach is required to solve the problem in a more practical way.

3.3 CONSIDERATIONS IN THE APPLICATION OF BUBBLES

A computer based literature search was performed and a listing made of report abstracts regarding the production of micron and submicron droplets. From the several hundred abstracts obtained, the reports of interest were narrowed to about 90, and those reports were ordered and studied. In those cases where micron and submicron droplets were made, the process involved: (1) dilution of a low vapor pressure liquid in a higher vapor pressure liquid which was then sprayed; (2) a condensation process in the expansion of a high Mach number flow; (3) electrohydrodynamic (EHD) spraying which produces droplets that are too highly charged as discussed above.

None of these methods was found to be suitable for application to the production of energy-economic drolets for EFD wind

driven generators. These difficulties have led to the concept of utilizing large air-to-water volume-ratio, bubbles, or hollow droplets. (As used here, hollow droplets correspond to extremely small bubbles). In the following, the studies made with regard to the application of bubbles will be discussed.

3.3.1 Emitter Opening Height

In the previous section, for the water to be emitted from the electrode as a sheet, the thickness was found to be 6×10^{-7} meters. Translating this thickness value into molecular diameters provides a number equal to about 1000. To replace this sheet of water of thickness Δh with a sheet of equally spaced thin wall bubbles having a wall thickness value of R, and the same volume of water, one can readily determine the ratio of bubble spacing (center to center), S, to bubble diameter, D, as follows. The volume of water in a sheet that is replaced by one bubble is

$$\text{Vol} = S^2 \, \Delta h$$

The volume of water in a thin wall bubble (thickness ΔR) is

$$\text{Vol} = \pi D^2 \cdot \Delta R$$

Equaling the two volumes and solving for the ratio S/D, one finds:

$$S/D = \sqrt{\pi \Delta R / \Delta h} \qquad (1)$$

where ΔR equals the bubble wall thickness. For the present example, inspection of the equation indicates that for bubble wall thicknesses of 100 molecules ($\Delta R = 5 \times 10^{-8}$ m) that the

bubbles would necessarily occupy more space than that of a two-dimensional slab of a thickness equal to the bubble diameter, again assuming the same amount of water. This is very favorable.

The major question of interest is, can the application of bubbles or hollow droplets provide adequate emitter slot dimensions? Again, considering Equation (1), the slot height needs to be at least as great as the bubble diameter, and control of bubble exiting velocity could permit slot heights equal to many bubble diameters and/or the use of several slots for each channel. In particular, geometries having lateral emission slots could use very low exiting velocities, since the wind would catch the bubbles and accelerate them to essentially the wind's velocity in a very short distance.

Conditions which limit bubble diameters will be considered in the following sections so that we can determine the largest possible diameter that can be used in our application.

3.3.2 Electrical Stability of Bubbles or Hollow Droplets

There are two regions in an EFD generator where electrical stability of a bubble or hollow droplet could be considered important. One is at the emitter where charging takes place and the second is at the entrance to the conversion section where the field is highest. Stability of water droplets and bubbles has been experimentally investigated early in this century by several researchers, notably Zeleny[18], Macky[19], and Wilson and Taylor[20]. Wilson and Taylor derived from their experiments of the stability of a half sphere on a wet grounded plate subjected to the influence of a uniform electric field, E, the expression for stability of a soap bubble in SI units as

$$E\sqrt{R} \leq 37{,}000 \qquad (2)$$

where R is the initial radius of the bubble. In the determination of Equation (2), they found that the limiting field, before the

bubble became unstable, was proportional to the square root of the surface tension. The value of surface tension that they measured for the soap solution they used was 0.028 N/m. Thus, the effective surface tension for a bubble, which has two surfaces, was 0.056 N/m. Wilson and Taylor calculated that the largest stable bubble in a field equal to the electrical breakdown value for normal atmospheric pressure to be 1.5×10^{-4} m radius, and for a pure water droplet to be 2×10^{-4} m radius. If we look at the case where the surface tension approachs that of pure water for a bubble (T = .157 N/m), then the largest stable radius would be twice as great as for the water drop or 4×10^{-4} meters. In the following, the stability considerations will be based on the lower surface tension value as used by Wilson and Taylor in their experiments.

Under the assumption that the stability relationship, Equation (2), holds for induction charging of bubbles emerging from a metal perforated plate, one can approximate the limiting charge to water mass ratio under atmospheric conditions as a function of the bubble's properties.

3.3.3 Bubble Charge to Water Mass Ratio Considerations

For the assumption that the bubble leaves a flat electrode in a uniform field in the bubble production and charging process, the charge on the bubble can be estimated as

$$q = C \Delta V \qquad (3)$$

where ΔV here is assumed to be the product of the field strength (corresponding to the potential and separation distance of the flat plate and its attractor electrode) and the bubble radius. C is the capacitance of the bubble. Solbes, in Reference (21), gives the value of the capacitance as

$$C = 4\pi\varepsilon R \alpha \qquad (4)$$

where he found a typical value for α to be of the order of 2 to 3. Cho's report (Reference (22)) provides an equation where the

corresponding value of α can be calculated as being equal to 1.65. Using the latter value,

$$q = 6.6\,\pi\varepsilon\ R\Delta V \tag{5}$$

and with

$$\Delta V = ER \tag{6}$$

$$q = 6.6\pi\varepsilon\ R^2\ E \tag{7}$$

Forming the charge to mass ratio, using

$$m = \rho_w 4\pi R^2\ \Delta R \tag{8}$$

$$\frac{q}{m} = \frac{1.65\varepsilon\ E}{\rho_w\ \Delta R} \tag{9}$$

As an example for water we have assumed the following values:

$$\rho_w = 1000\ kg/m^3$$

$$\frac{q}{m} = .03\ \frac{C}{kg}$$

$$\Delta R = 5 \times 10^{-7}\ m$$

$$\varepsilon = 8.9 \times 10^{-12}\ c/m\text{-}V$$

Thus, the electric field required to charge the bubbles is $E = 1 \times 10^6$ V/m. This value is one third the breakdown strength of air and, therefore, is a favorably low value.

Another test for stability, in addition to that of Wilson and Taylor, is the application of Rayleigh's equation for the limiting charge on a droplet, i.e.,

$$q = 8\pi(T\varepsilon)^{1/2}\ R^{3/2} \tag{10}$$

and for a bubble with two surfaces, we have:

$$q = 8\pi(2T\varepsilon)^{1/2} R^{3/2} \tag{11}$$

Dividing through by the mass of a bubble yields:

$$\frac{q}{m} = \frac{2(2T\varepsilon)^{1/2}}{(R)^{1/2} \Delta R \rho_w} \tag{12}$$

where for the same value of surface tension as used by Wilson and Taylor, ($T = 0.028$ N/m) and the previously assumed values of q/m of .03, and of ΔR of 5×10^{-7} m, one can solve for the largest stable value of R:

$$R \leq .0087 \text{ m} \tag{13}$$

Bubbles much smaller than this radius can be readily made, so that Rayleigh's charge limit can be dismissed as a limitation.

The above considerations make it appear reasonable that the application of Equation (2) for the stability of a bubble is appropriate for the emitter region. For the case under consideration, the charging field was calculated to be 1×10^6 V/m. Applying this value to Equation (2) and solving for the limiting value of R gives:

$$R \leq .0014 \text{ m} \tag{14}$$

This value of radius corresponds to a small, but practical size bubble diameter.

In the entrance portion of the conversion section, the maximum field should approach the value corresponding to breakdown, or $E = 3 \times 10^6$ V/m. Again, applying the stability expression of Equation (2) yields,

$$R \leq 1.5 \times 10^{-4} \text{ m} = 150 \ \mu\text{m} \tag{15}$$

and this is a very small bubble--a hollow droplet. It is not

known whether such small bubbles have ever been made, but before their application can be ruled out, other considerations fundamental to the EFD process will be made in the following.

Electrical breakdown of the air near the surface of the drops presents another consideration. A particle placed in an insulating medium having a uniform field, E_1, causes a change in the electric field at the particle's surface. It is of interest to examine theoretically the effect of the charge on this field. For the case of a conductive sphere of charge q, the net electric field, E, at any point on the sphere, following White[23], is

$$E = 3E_1 \cos\theta - \frac{q}{4\varepsilon\pi R^2} \tag{16}$$

where θ is the angle from the polar axis which is aligned with the field. The largest absolute value for the field is

$$E = \left| 3E_1 + \frac{q}{4\varepsilon\pi R^2} \right| \tag{17}$$

Introducing the charge to water mass ratio parameter (q/m) and setting E equal to the breakdown strength of air, E_b, and solving for E_1/E_b we have

$$\frac{E_1}{E_b} = \frac{1}{3} - \frac{q}{m}\frac{\rho_w \cdot \Delta R}{3\varepsilon E_b} \tag{18}$$

Note that the radius of the hollow droplet has cancelled out. Local values of E_b have been found to be a function of the radius for very small dimensions, and these breakdown values are far larger than the commonly accepted value. Therefore, we will assume the value commonly accepted which is conservative. For the

previously assumed values $q/m = .03$ C/kg, $\rho_w = 1000$ kg/m^3, and $\Delta R = 5 \times 10^{-7}$ m, we have:

$$\frac{E_1}{E_b} = \frac{1}{3} - \frac{1.4 \times 10^5}{E_b} = .286 \qquad (19)$$

For E_b equal to 3×10^6 V/m the effect of the charge is seen to be small so that the empirically derived equation by G. I. Taylor could be applicable ($E_1 \sqrt{R} \leq 37{,}000$) as equation (19) would provide $E_1/E_b = 1/3$ for the case of no charge on the droplet.

3.4 MOBILITY OF CHARGED HOLLOW DROPLETS

At this point we have not shown that hollow droplets can not be used as charge carriers in the high electric field section of the generator; namely, at the entrance to the conversion section. Droplets as large as 300 μm in diameter could be stable, as discussed in the preceeding sections. However, considerations of droplet mobility and energy costs remain to be made.

In Reference (1) (page 46), the mobility of charged droplets (the drops were not hollow) was plotted versus the droplet radius for many values of the curve parameter, q/m, or charge to water-droplet-mass ratio.

The equation describing mobility, k, which was plotted was

$$k = \frac{(q/m) \quad m}{6\pi\mu R} \left[1 + L/R + (A + Be^{-CL/R})\right] \qquad (20)$$

and values of droplet radius were varied over the range of 10^{-8}m to 10^{-5}m. According to Decaire[24], Equation (20) was empirically derived by Millikan and others and is valid for intermediate size droplets: from ions up through droplet sizes which follow Stokes Law. For droplets larger than 10^{-6}m radius, Stokes Law for the

drag of a particle applies. Following Decaire for the derivation of mobility of larger droplets[24], the drag force of the droplet is equated to the electrical force,

$$q \cdot E = 6\pi\mu R v$$

In this equation, v, is the equilibrium velocity and u is the coefficient of viscosity of the gas. Now the definition of mobility is in terms of the equilibrium velocity and the electric field:

$$k = \frac{v}{E}$$

Therefore,

$$k = \frac{(q/m) \quad m}{6\pi\mu R} \tag{21}$$

For a hollow droplet we have

$$m = \rho_w \cdot 4\pi R^2 \cdot \Delta R \tag{22}$$

So that,

$$k = \frac{2}{3} \frac{q}{m} \frac{\rho_w \Delta R \; R}{\mu} \tag{23}$$

Taking the viscosity, μ, of air to be 1.8×10^{-5} N-s/m^2 and the density of water as 1000 kg/m^3,

$$k = 3.70 \times 10^7 \cdot q/m \cdot \Delta R \cdot R \tag{24}$$

One notes that the mobility is proportional to the charge to water mass ratio, to the film thickness of the hollow droplet and, most importantly, to the radius of the droplet. Equation (24) is plotted in Figure 3 for ΔR equal 5×10^{-7} meters.

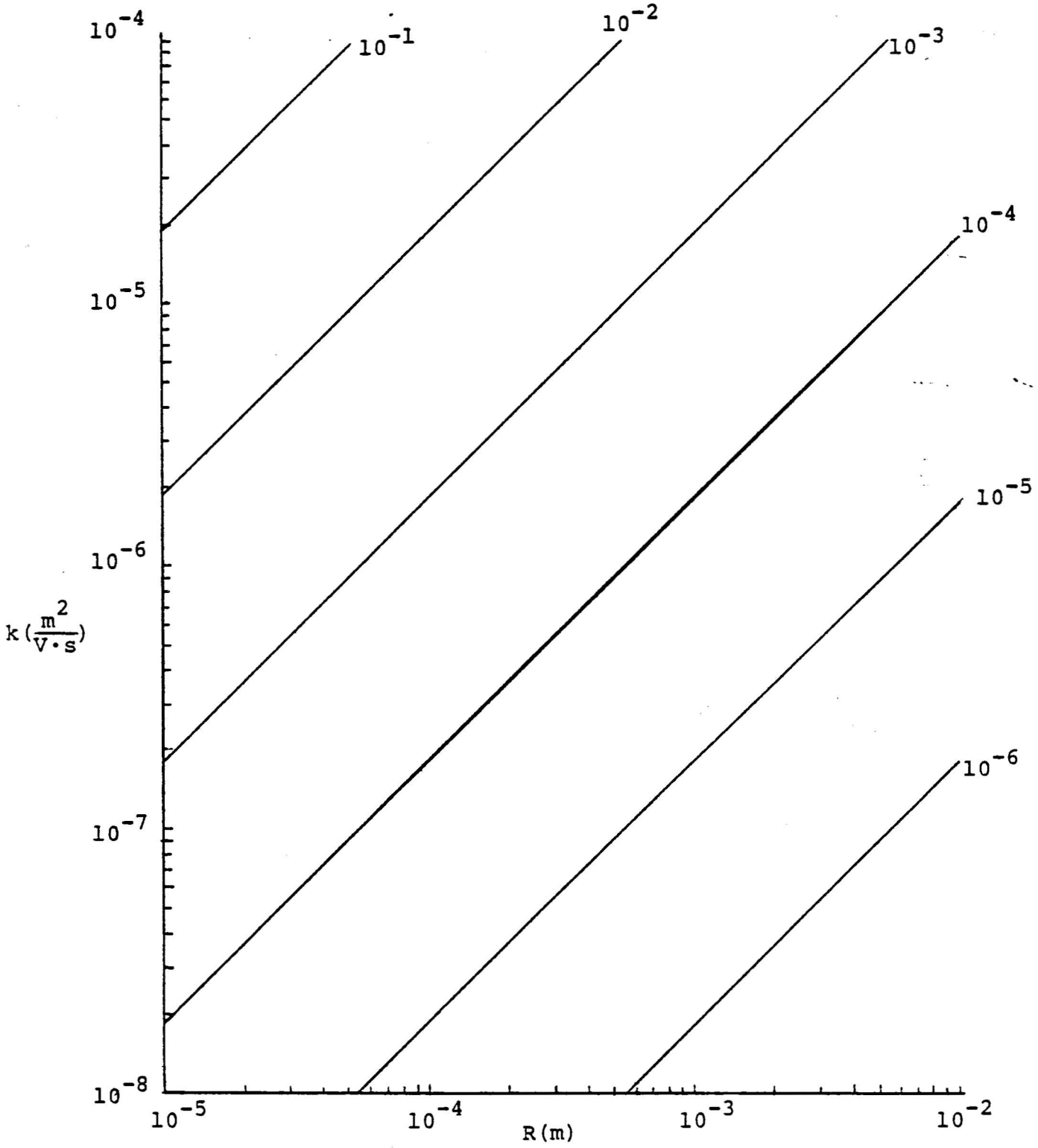

Figure 3. Theoretical Mobility vs. Hollow Droplet Radius. Curves parameterized by charge to water mass ratio. The value of ΔR taken for the film thickness is 5×10^{-7} m.

3.5 WORK REQUIRED TO FORM HOLLOW DROPLETS

The work in forming droplets (nonhollow) was analyzed in Reference (2). It was determined that there were three major categories of work: power to form droplet surfaces, power to charge the surfaces, and power to pump the water to the required pressure. As the purpose of the droplets is to effectively carry charge to the collector, a ratio was formed corresponding to work (a product of charge and voltage: C · V) per coulomb of transported charge, or volts. This is an especially worthwhile parameter since the collector voltage must exceed this voltage to get net power out of the EFD generator. The ratio of the work per coulomb, or voltage, to the collector voltage is the fraction of the generator's gross power that must be used to produce the required work in the given category.

3.5.1 Surface Tension Energy Costs

The work surface tension energy in a hollow droplet which has two surfaces is

$$w_s = 2T(4\pi R^2) \tag{25}$$

with

$$m = \rho_w \, 4\pi R^2 \, \Delta R$$

$$w_s = \frac{2T \, m}{\rho_w \, \Delta R}$$

Dividing both sides of the equation by the charge, q,

$$\frac{W_s}{q} = \frac{2T}{\Delta R \rho_w (q/m)} \tag{26}$$

As in Reference (2), by applying Equation (23), one can provide an explicit relationship between the hollow droplet radius,

mobility, and the work per coulomb for given T and μ.

$$\frac{W_s}{q} = \frac{4}{3}\frac{TR}{\mu k} \tag{27}$$

with $$\mu = 1.8 \times 10^{-5}$$

$$\frac{W_s}{q} = \frac{7.41 \times 10^4 \cdot T \cdot R}{k} \tag{28}$$

This equation is plotted in Figure 4, where the value of surface tension was taken as 0.0735 N/m for water.

For a hollow droplet having a very small radius of 5×10^{-5} meters, and a mobility value in the favorable range of

$$k = 1 \times 10^{-6} \text{ to } 1 \times 10^{-7} \text{ m}^2/\text{V-s}$$

one reads from the plot, respectively,

$$W_s/q = 2.7 \times 10^5 \text{ to } 2.7 \times 10^6 \text{ V}$$

Both of these values are excessively large for hollow droplets to be used as charge carriers in the generator conversion section. Although this study shows that the application of hollow droplets as low mobility charge carriers is not feasible, due to the high value of work per coulomb calculated for surface tension energy costs, the other major costs will be considered in the following sections for the sake of completeness.

3.5.2 Water Pumping Costs

The basic expression for this cost is unchanged from that in Reference (8), i.e.,

$$w_p = P_p \cdot \text{Vol} = P_p \cdot \frac{m}{\rho_w}$$

where Vol equals the volume of water and P_p equals the pressure rise across the pump. Dividing both sides of the above equation by the charge, q,

$$\frac{W_p}{q} = \frac{P_p}{w(q/m)} \tag{29}$$

and, again, q/m can be related to the mobility, as above,

$$\frac{W_p}{q \cdot p} = \frac{3.7 \cdot 10^4 \cdot \Delta R \cdot R}{k} \tag{30}$$

Expressing the pressure, P, in atmospheres,

$$\frac{W_p}{q \cdot p} = \frac{3.75 \quad 10^9 \ \Delta R \ R}{k} \tag{31}$$

and this cost is also plotted in Figure 4.

As in the previous section, considering a hollow droplet having a radius of 5×10^{-5} meters and a mobility value in the range of

$$k = 1 \times 10^{-6} \text{ to } 1 \times 10^{-7} \ m^2/v\text{-}s$$

one reads from the plot

$$\frac{W_p/q}{P_{atm}} = 9.4 \times 10^4 \text{ to } 9.5 \times 10^5$$

For the water to be pumped to a pressure level corresponding to three atmospheres,

$$W_p/q = 2.8 \times 10^5 \text{ to } 2.8 \times 10^6$$

These values are nearly identical to the surface tension energies per coulomb of charge and are also excessively high.

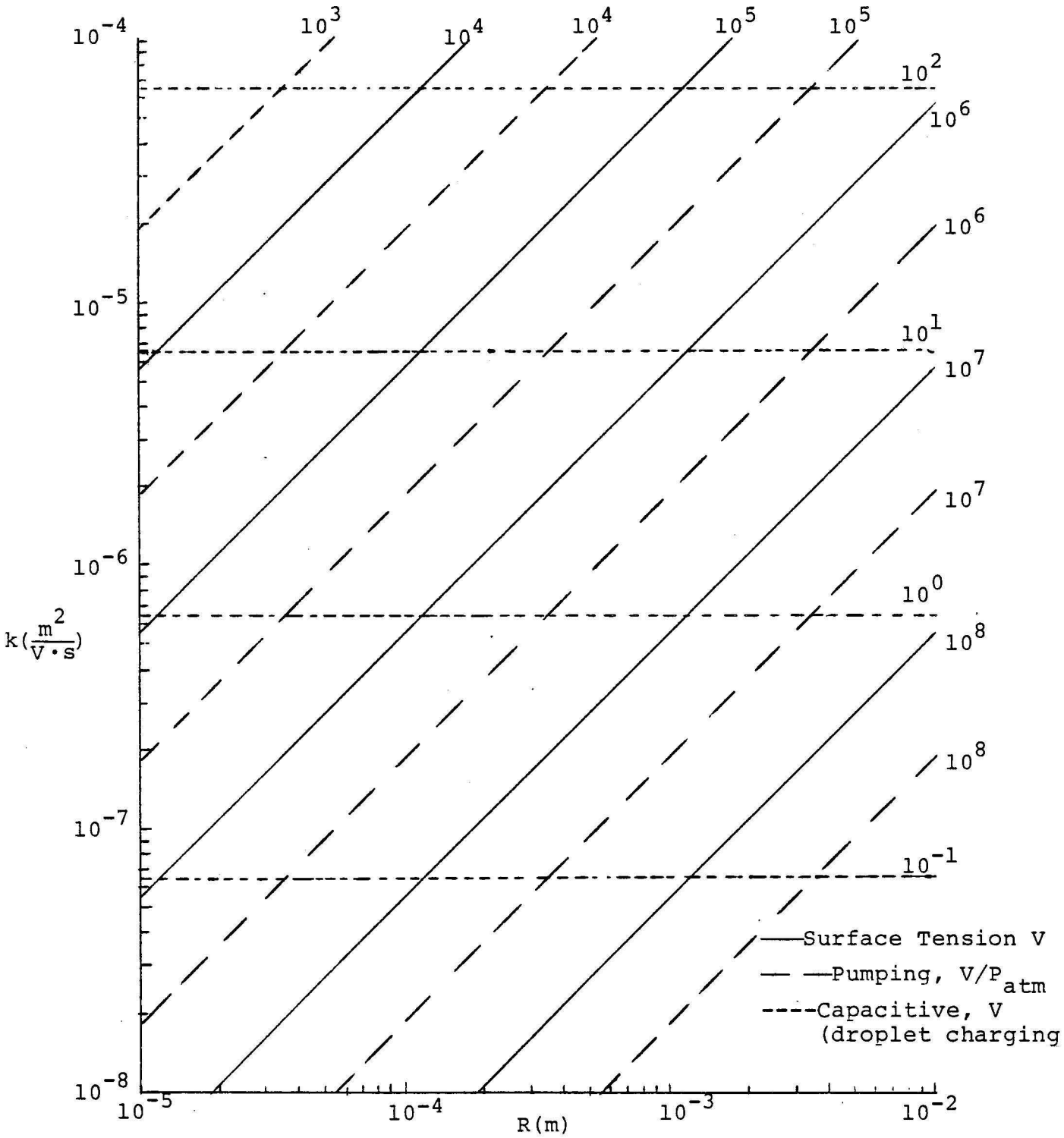

Figure 4. Specific Charged Hollow Droplet Energy Cost (Joule/Coulomb) of Collected Charge Plotted in the Mobility-Droplet Radius Plane.

3.5.3 Electric Charging Energy Costs

According to Reference (25), the potential energy corresponding to the charge on a sphere is:

$$W_c = \frac{q^2}{8\pi\epsilon R} \tag{32}$$

Forming the electric charging energy cost ratio for a hollow droplet,

$$\frac{W_c}{q} = \frac{q}{m}\frac{\rho\Delta R\ R}{2\epsilon} \tag{33}$$

Substituion for q/m, as before,

$$\frac{W_c}{q} = \frac{3k\mu}{4\epsilon_o} \tag{34}$$

$$\frac{W_c}{q} = 1.52 \times 10^7\ k$$

The above equation is also plotted in Figure 4 for several values of the parameter, charging work per coulomb of charge, W_c/q. One notes that this work varies proportional to the mobility. For the aforementioned range of suitable mobility, namely,

$$k = 1 \times 10^{-6} \text{ to } 1 \times 10^{-7}\ m^2/V\text{-}s$$

$$W_c/q = 15 \text{ to } 1.5\ V$$

These values are negligible in comparison to the several hundred thousand volts that EFD generators will produce.

3.6 CONCLUSIONS ON THE APPLICABILITY OF BUBBLES AND HOLLOW DROPLETS TO EFD GENERATORS

Considerations of the water distribution problem for forming charged droplets and the inapplicability of electrohydrodynamic spraying for the production of low mobility charged droplets has led to the investigation of the induction charging of bubbles. Analyses indicate practical-size bubbles, and emitter slots as well as favorably low charge-to-water mass ratios can be achieved by the induction charging method. Further, the mobility-energy cost analyses definitely show that the bubbles can be applied only as part of the charged droplet production process in that they can not serve as charge carriers in the generator conversion section. Thus, a means (during or immediately after the forming of the charged bubble) will be necessary to cause the bubbles to break up into essentially uniform micron or submicron size charged droplets.

The use of bubbles can provide practical size emitter slots or widths up to many bubble diameters. Rather large bubbles are stable only in the charging regime, while small bubbles or "hollow droplets" may be stable also in the high field region of the conversion section. However, the latter are not energy cost effective as low mobility charge carriers. Thus, only large bubbles should be considered along with a means to break them up into uniform-sized, small droplets. A study conducted in Reference (2) indicates that the surface tension energy of micron and submicron droplets can be provided in bubbles of sufficiently low film thickness, on the order of 5×10^{-7} meters. Thus, a process to shatter bubbles may not require significant energy input. Although it is not understood at the present how to disrupt the bubbles, one possible method may be the collision of charged or uncharged bubbles with a very open mesh screen in the presence of an electric field. In this way, the bubbles could be caused to disintegrate into charged droplets.

SECTION 4
EXPERIMENTAL INVESTIGATIONS

4.1 INTRODUCTION

The experimental investigations of the application of bubbles for the proper distribution and charging of water to provide energy economic, low mobility, charged droplets has required the design and fabrication of a new large electrode generator test apparatus. The entrance electrode lattice of the old generator was made up of twelve 1.59×10^{-2} m (5/8 in) diameter electrodes which provided eleven flow channels. It was desired to reduce the number of flow channels to three where, for the energy economic charging experiments, only the center channel would be provided with electrical charges.

This would reduce the complexity of the testing yet provide representative flow conditions. Thus, while the major objective was the development and demonstration of an energy economic charged droplet production method, preliminary objectives were the design, construction, and testing of a large-diameter-element, four-electrode entrance geometry. It was believed that testing this new geometry, using the previously proven method of making low mobility charge droplets, which although energy uneconomic, could provide baseline operational characteristics to aid in judging the new bubble charging methods. In addition, other supporting objectives were the design and construction of a bubble generator and bubble emitter geometries.

4.2 LARGE DIAMETER ELEMENT ENTRANCE ELECTRODE DESIGNS

To facilitate the testing of a new method for the production of energy economic charge droplets it is advantageous to use generator geometries having large electrodes, as this reduces the number of emitter rows and channels. This in turn provides the highest flow rates of water per unit length of electrode.

Testing is done in a wind tunnel having a square test section 0.91 m by 0.91 m (3 ft by 3 ft), and this corresponds to an area four times larger than the generator test array. It was decided to leave the generator collector unchanged as it could perform satisfactorily for charge emitters having the same length as the previously used ones. The twelve electrodes, making up the old attractor array, were cylindrical and were 0.0159 m (5/8 in) in diameter. As the array was 0.457 meters across, this provided an electrode spacing to diameter ratio, a, of 2.53. As discussed in previous reports, this is a characteristic dimension and it was decided to maintain this value for the new large electrodes. Further, as stated earlier, it was desired to reduce complexity as much as possible by testing a single emitter. However, in order to provide representative flow conditions for the single emitter channel, bordering flow channels should be provided. The above considerations led to a four element (three channel) attractor design made up of 0.051 m (2 in) metal cylinders with a centerline spacing of 0.128 m (5.06 in).

The research plan called for the testing of the large electrode design with the previously used droplet forming and charging system, which is fully described in Reference (2). Briefly, the method can be be described as follows. The air is brought to nearly 100 percent saturation and is then chilled as it approaches the test array by a spray of liquid nitrogen. Extremely small drops of water are formed by condensation which subsequently are charged by corona. This method, although not energy economic, has provided design levels of current of the required low mobility and has allowed the successful verification of EFD wind generator theory. For the first large electrode generator performance experiments using the proven corona method, all three channels could be operated with charged droplets without significant increase in complexity. Figure 5 is a picture of one of the corona charging, large electrode designs. Three corona wires, one for each channel, are supported by an

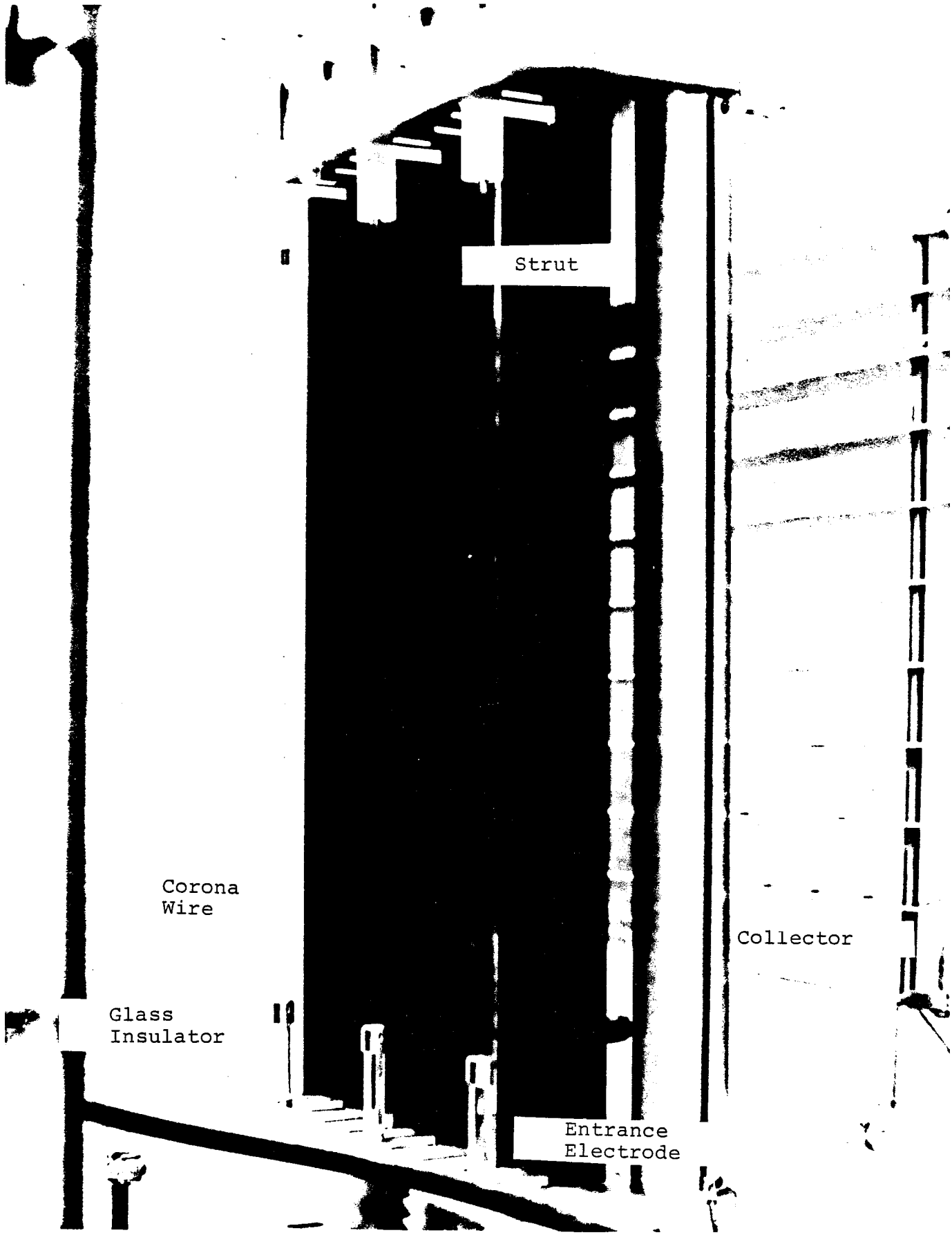

Figure 5. First Large Electrode Geometry Rig.

individual tubular glass insulator at the bottom plate. The glass insulators have a rounded cylindrical cap in which the corona wire is anchored with a setscrew. The upper ends of the wires are supported by a common metal plate which rests on two lexan cylindrical insulators. The three wires are attached to fittings at the upper ends of 6.35×10^{-3} m (.25 in) stainless steel tubes. The wires are held on the centerline of the tubes. The tubes have a far larger diameter and, therefore, have a greatly reduced field at their surfaces over that which the wires would incur in their passage through the openings in the large flat plate. To further increase the maximum operating potential, the three metal tubes were sheathed in polyethylene cylinders, as seen in the picture. The power supply cable is seen at the top surface of the flat plate which supports the corona wires.

The corona wires are followed, in the flow direction, by pairs of black electrodes which are streamline-strut-shaped and are 1.9×10^{-2} m (.75 in) at their widest point and 3.65×10^{-2} m (1 7/16 in) in length. The three pairs of struts serve as attractor electrodes and are on centerlines spaced 5.7×10^{-2} m (2.25 in) apart. The function of the struts is to allow operation with a reduced power supply voltage since they are much nearer to the corona wires than the large entrance electrodes. Both the struts and corona wires are mounted in axial slots so that they can be moved away from or toward the plane of the four large circular entrance electrodes. The field created by the corona wires and struts tend to accelerate and broaden the charge cloud in the region upstream of the struts. Within the struts, the charge cloud thickens due to turbulence and space charge field effects. For suitably-low-mobility droplets, the charge cloud width at the exit plane of the struts can be smaller than the strut spacing so that no charged droplets are lost to the electrodes. Immediately downstream of the struts, the space charge field is anchored primarily on the trailing surfaces of the struts, while the field of the space charge further

downstream in the conversion region is anchored primarily on the large entrance electrodes.

Maximum current tests were conducted for the collector at ground potential. These tests yielded generator current values of 315 microamps or about 60 percent of the maximum value of current achieved with the small diameter electrode attractor array.

Several corona wire attractor electrode configurations were tested in an attempt to increase the current level or to provide a basis for explaining this 40 percent reduction of current. The geometry pictured in Figure 6 produced a current of 340 microamps. It was the only geometry tested that produced a higher value of collected current than the first geometry. In the geometry of Figure 6, a third strut is placed directly in front of the corona wire so that the wire is in the strut's wake. The premise underlying this design was that the application of only three corona wires, in comparison to the eleven corona wires in the small electrode generator design, resulted in higher average fields not only at the surfaces of the wire, but also in the region where the ions were attaching to the droplets. The wake producing electrode ahead of the corona wire could shift the bulk of the droplet laden flow into a somewhat lower field region so that on the average, fewer ions would attach to a droplet. Although the change in current resulting from this geometry was small, it was positive.

In the experiments discussed above, the collector was spaced 1.01×10^{-2} m (4 in) downstream of the rear plane of the large diameter electrodes. This is the same spacing as was used for the small electrode geometry. Thus, at first thought, one might expect similar field strengths for the charged droplet flow in its passage through the conversion section. However, EFD scaling laws indicate that the current density scales inversely with electrode size while the output voltage scales directly proportional to electrode size. Strict adherence to the scaling

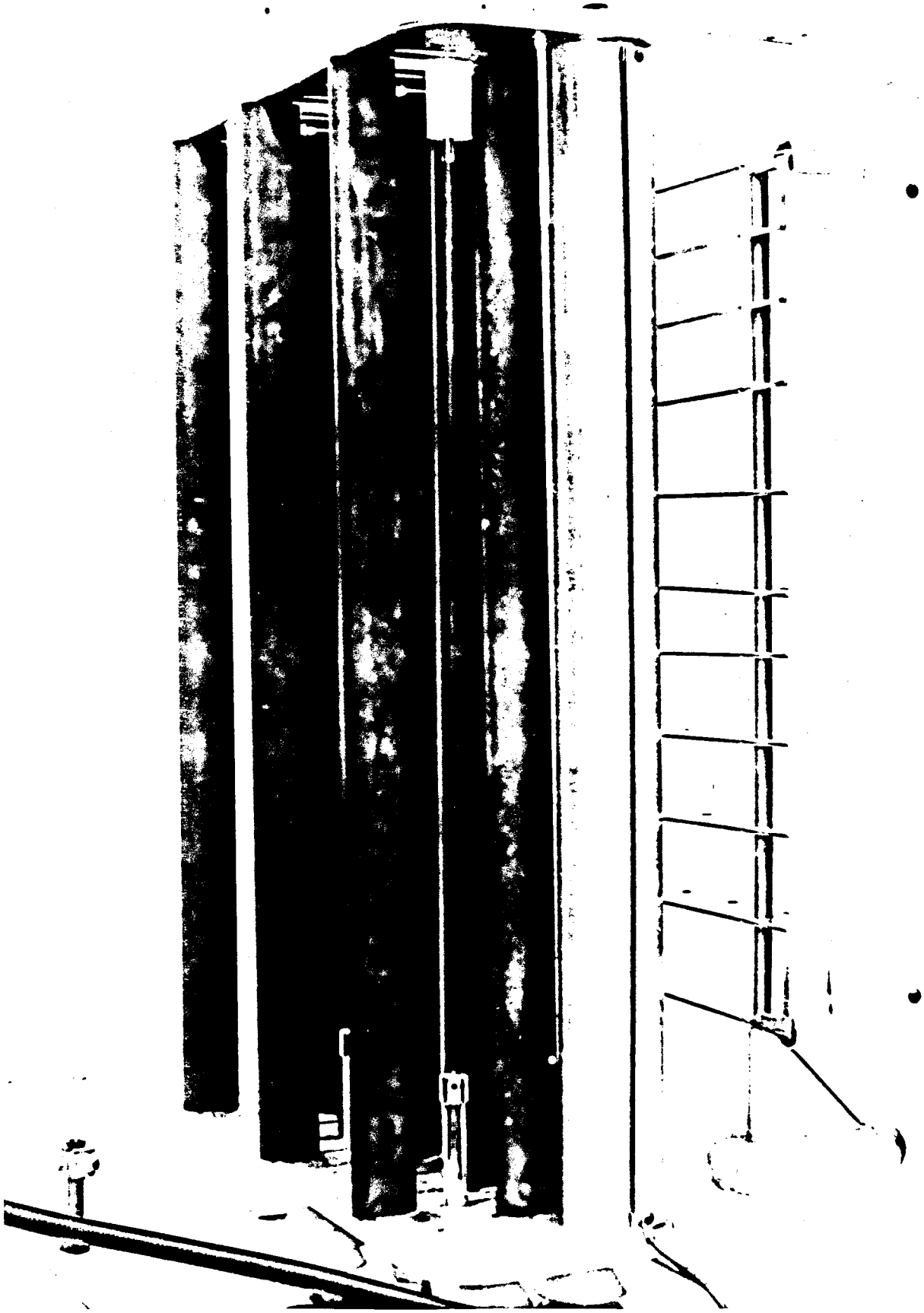

Figure 6. Electrode Geometry that Produced the Maximum Current of 340μ.

laws would provide equal values of maximum field as well as similar field structure. Thus, another reason for the low value of maximum current may be that the current level of 340 microamps corresponds to the attainment of field strengths equal to breakdown in the new configuration and thus is a true limit. This possibility should be checked out using the UDRI field solution computer program. Computer results may indicate a longer conversion section is necessary to achieve design performance.

4.3 DESIGN OF A HIGH CAPACITY BUBBLE GENERATOR

Commercial foam generator brochures were reviewed to determine the possiblity of purchasing a suitable off-the-shelf item. However, as the application of these generators is directed toward fire fighting, the smallest size generator available is far too large. Thus, it was decided to design a bubble generator that would have a great amount of flexibility, both with regard to volume flow and bubble characteristics.

A review of the literature provided two basic designs. In one design, a liquid is sprayed onto a screen, and a blower forces air through the wetted screen, causing bubbles to come off the downstream side. In the second design, no blower is used, but a spray of liquid powers and wets a ducted airstream which is directed through a screen. The wetted screen then produces bubbles, as in the design discussed previously. Although the second method might be preferable for practical application in the future, the first method was selected as it provided control over the air flow characteristics.

The major components of the bubble generator which was designed and fabricated are a radial blower, a plenum chamber with adjustable bleed valves, an outlet duct containing a "fuel spray" nozzle, a screen to receive the liquid spray, and a transition duct providing a path to the bubble emitter electrode. The volume flow of air to the emitter is controlled by adjustment of the bleed values on the plenum chamber. Also, the

screen size can be varied to match flow velocity requirements across the screen. Figures 7 and 8 provide two different views of the bubble generator in position under the wind tunnel.

4.4 BUBBLE EMITTER ELECTRODE DESIGN

As discussed earlier in this section, only one emitter electrode was to be applied in the energy-economic charged droplet experiments. In the large electrode geometry, the center flow channel would receive the emitter electrode and the two neighboring channels would provide bordering, nearly similar flows.

Two different emitter electrodes were designed and fabricated. One emitter electrode has a slot in the trailing edge of the electrode where the bubbles enter the flow. The position of the attractor electrode is such that the electric field at the exit is predominately an axial field: the field lines are parallel to the air flow direction. The second emitter electrode has two slots: one on each side of the air foil shaped electrode. The attractor electrodes are positioned opposite the emitter slots and, therefore, produce an electric field which is predominately a lateral electric field: the field lines are perpendicular to the airflow direction. The two emitters were similar in other design aspects.

The sidewall emitter slot is pictured in Figure 9. In the first experiments, the emitter body was purposely oversized in order to ensure a sufficient volume flow from the bubble generator, positioned directly under the test apparatus. The vertical feed tube is 0.102 m (4 in) in diameter and the airfoil section is about 0.306 m (1 ft) in length. In the picture, the front edge of one emitter slot is almost on a line with an adjacent strut which serves as an attractor electrode. The slot is 1.27×10^{-2} m (0.5 in) by .457 m (18 in). The attractor electrodes are 2.86×10^{-2} m (1 1/8 in) distant on either side of the emitter. A short straight wall section follows each slot,

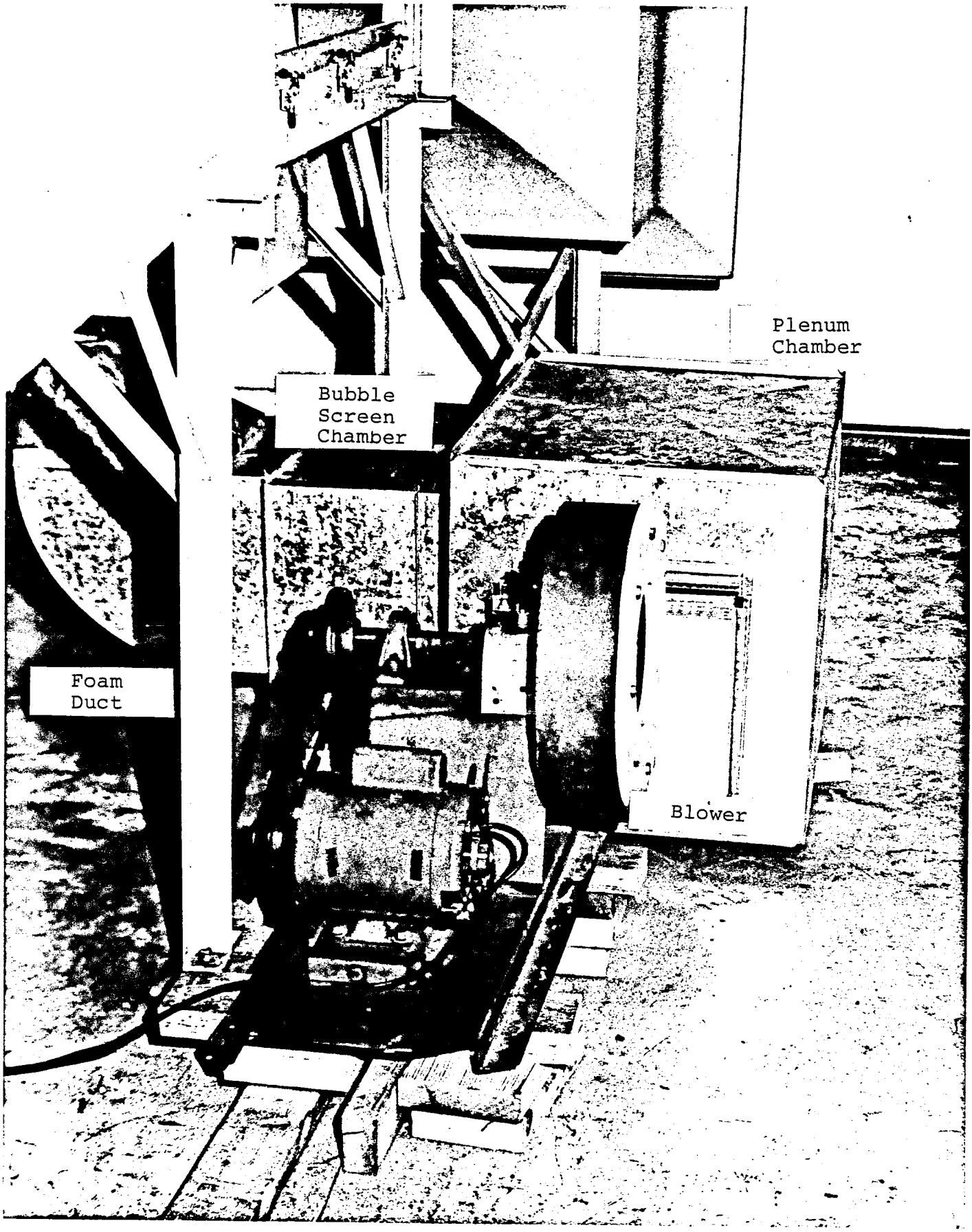

Figure 7. Bubble Generator.

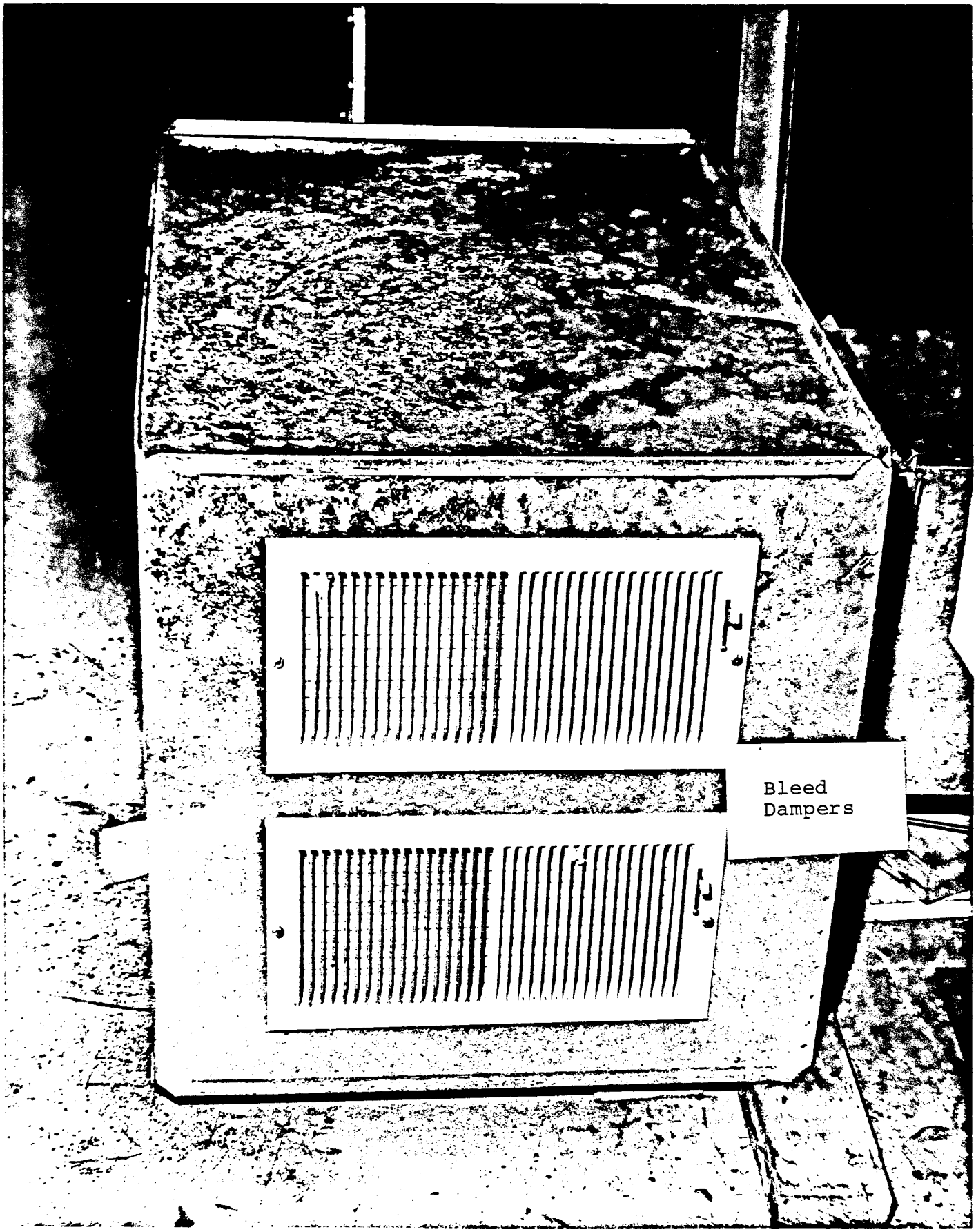

Figure 8. Bubble Generator Plenum Chamber.

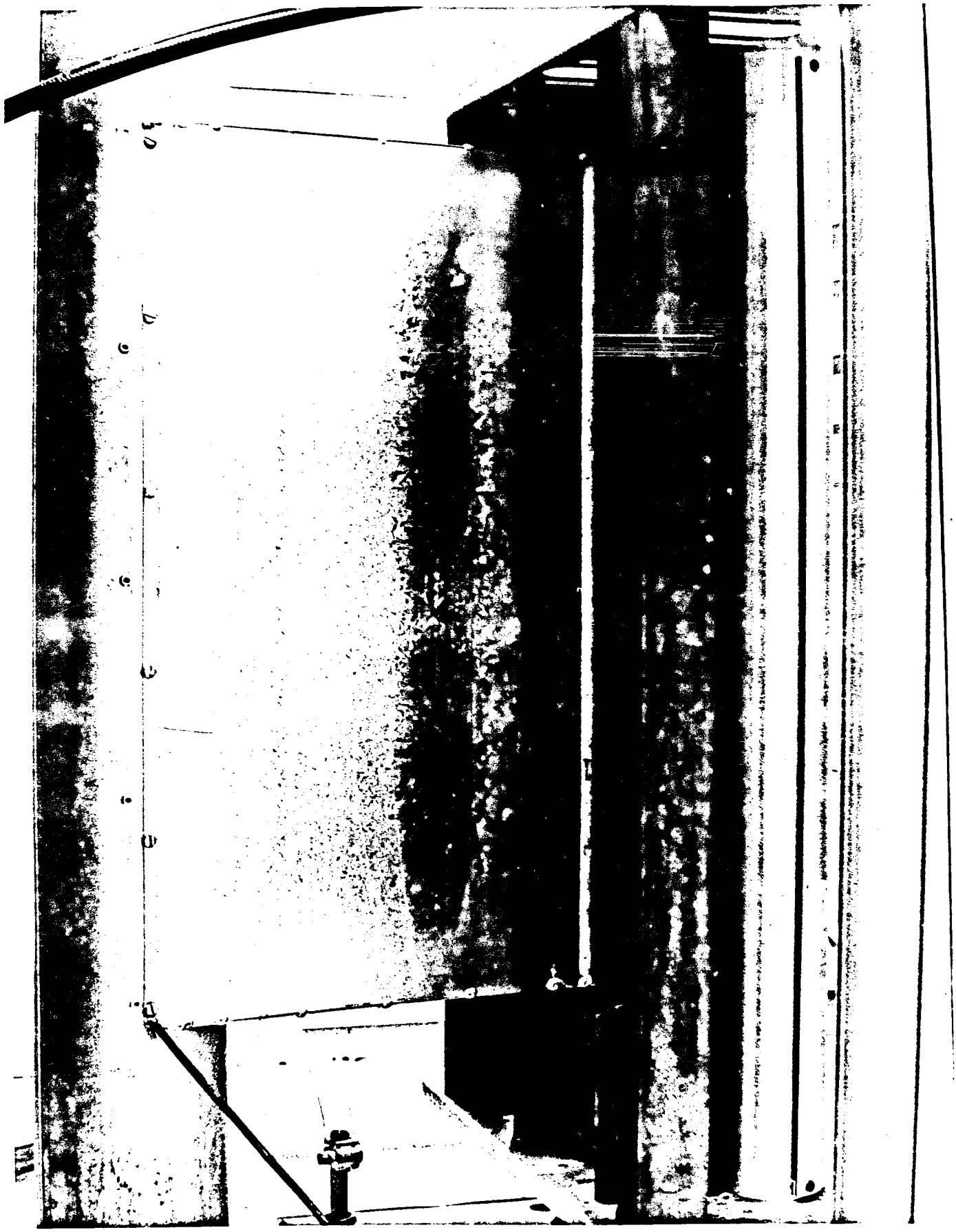

Figure 9. Bubble Emitter Electrode Geometry.

followed by a 1.27×10^{-2} m (0.5 in) radius section which forms the trailing "edge" of the emitter. The trailing edge should not be sharp as in a typical airfoil because of electric field intensification considerations.

Preliminary tests have been conducted. Although at this time, a uniform flow of bubbles over the height of the slots has not been realized, a satisfactory emitter current level of 250 microamps was measured. The attractor voltage was moderate, corresponding to a field strength of 175×10^3 V/m. This value is about 20 percent of that calculated for the specific theoretical example considered in Section 3.3.3.

From the theoretical investigation discussed in Section 3, it was shown that the charged bubbles would be required to burst into small size charged droplets, in order to provide satisfactory, low mobility charged droplets. This will require additional experiments and perhaps simpler, more basic, test geometries.

The results of both the experimental program and theoretical studies have been very encouraging. These results have clearly indicated a future program direction which will be most likely to lead to an energy-economic method of charge production. A brief outline of our future plans are given in the next section.

SECTION 5
FUTURE PROGRAM PLANS

Experimental investigations of the large electrode geometry conducted during the last year have shown the need to calculate performance characteristics utilzing UDRI's computer program. This appears to be particularly important when making large changes in electrode dimensions as was done during the last year. Formerly, the channel widths were small in comparison to the conversion channel length so that the flow could be treated satisfactorily, applying the quasi-one-dimensional theory, developed earlier.

It was also learned that the field structure should be determined in the neighborhood of the emitter as well as downstream through the entrance electrode and through the conversion section to the collector, rather than studying the conversion section field strength only, as most investigators have done.

A major effort is required in the experimental investigations of the production, charging, and disintegration of thin wall bubbles. Two types of experiments are planned. One will use laboratory bench type experiments to investigate simple basic models where diagnostic tools can be used most advantageously; the other will use integrated-concepts in the large electrode generator where overall performance characteristics can be determined readily.

REFERENCES

1. Minardi, J. E., M. O. Lawson, and G. Williams, Electrofluid Dynamic (EFD) Wind Driven Generator, Final Report, COO/4130-77-1, October 1976, pp. 17-33, 54-61.

2. Minardi, J. E., M. O. Lawson, and F. L. Wattendorf, Third Annual Progress Report on the Electrofluid Dynamic Wind Generator, COO/4130-2, UC-60, May 1979, pp. 15-20.

3. Minardi, J. E., M. O. Lawson, and G. Williams, Electrofluid Dynamic (EFD) Wind Driven Generator, Final Report, COO/4130-77-1, October 1976, pp. 17-33, 33-41.

4. Ibid., pp. 65-73.

5. Ibid., pp. 65, 70, 71.

6. Ibid., pp. 29-33.

7. Ibid., pp. 43-53.

   Minardi, J. E., M. O. Lawson, and F. L. Wattendorf, Third Annual Progress Report on the Electrofluid Dynamic Wind Generator, COO/4130-2, UC-60, May 1979, pp. 19-30.

8. Minardi, J. E. and M. O. Lawson, "Progress in Electrofluid Dynamic (EFD) Wind Driven Generator Research," Third Annual Wind Energy Workshop, May 1978, Vol. 2, pp. 843-845, 849.

9. Minardi, J. E., M. O. Lawson, and G. Williams, Electrofluid Dynamic (EFD) Wind Driven Generator, Final Report, COO/4130-77-1, October 1976, p. 75.

   Minardi, J. E., M. O. Lawson, and F. L. Wattendorf, Third Annual Progress Report on the Electrofluid Dynamic Wind Generator, COO/4130-2, UC-60, May 1979, pp. 38-43, 51-58.

10. Minardi, J. E., M. O. Lawson, and G. Williams, Electrofluid Dynamic (EFD) Wind Driven Generator, Final Report, COO/4130-77-1, October 1976, pp. 75-79.

    Minardi, J. E., M. O. Lawson, and F. L. Wattendorf, Third Annual Progress Report on the Electrofluid Dynamic Wind Generator, COO/4130-2, UC-60, May 1979, pp. 58-60.

11. Minardi, J. E., M. O. Lawson, and G. Williams, Electrofluid Dynamic (EFD) Wind Driven Generator, Final Report, COO/4130-77-1, October 1976, p. 80.

12. Minardi, J. E., M. O. Lawson, and F. L. Wattendorf, Third Annual Progress Report on the Electrofluid Dynamic Wind Generator, COO/4130-2, UC-60, May 1979, pp. 41-43.

13. Ibid., 44-45.

14. Ibid., 51-54.

15. Ibid., 54-58.

16. Vonnegut, B., and R. L. Neubauer, "Production of Monodisperse Liquid Particles by Electrical Atomization," Journal of Colloid Science, No. 7, p. 616, 1952.

17. Minardi, J. E., M. O. Lawson, and F. L. Wattendorf, Third Annual Progress Report on the Electrofluid Dynamic Wind Generator, COO/4130-2, UC-60, May 1979, p. 29.

Minardi, J. E., M. O. Lawson, and G. Williams, Electrofluid Dynamic (EFD) Wind Driven Generator, Final Report, COO/4130-77-1, October 1976, p. 46.

18. Zeleny, J., "On the Conditions of Instability of Electrified Drops, with Applications to the Electrical Discharge from Liquid Points," Proceedings of the Cambridge Philosophical Society, Vol. 18, 1915.

19. Macky, W. A., "Some Investigations of the Deformation and Breaking of Water Drops in Strong Electric Fields," Proceedings of the Royal Society, A Vol. 133, 1931.

20. Wilson, C. T. R. and G. I. Taylor, "The Bursting of Soap-Bubbles in a Uniform Electric Field," Proceedings Cambro Phi. Soc. XXII, 728, 1925.

21. Solbes, A. and M. Martinez, Research on Charged Alkali Colloids for Aerospace Vehicle and Ground Based Power Generation, Final Report, ARL-TR-75-0004, February 1972-February 1974.

22. Cho, A. Y. H., "Contact Charging of Micron-Sized Particles in Intense Electric Fields," Journal of Applied Physics, Vol. 35, 9, pp. 2561-2564, September 1964.

23. White, H. J., "Industrial Electrostatic Precipation, Addision-Wesley Publishing Co., Inc., p. 132, 1963.

24. Decaire, J. A., The Effects of Partial Condensation Around Ions in Electric Fluid Dynamic Energy Conversion Process, ARL-66-0187, September 1966.

25. Pfeifer, R. J., "Parametric Studies of Electrohydrodynamic Spraying," Department of Electrical Engineering, Engineering Experiment Station, University of Illinois, Urbana, Illinois, Report No. CPRL-4-65.